

# Velocity distributions in clusters of galaxies

Andreas Faltenbacher and Juerg Diemand

*UCO/Lick Observatory, University of California at Santa Cruz, 1156 High Street, Santa Cruz, CA 95064, USA*

Accepted 2006 March 30. Received 2006 March 29; in original form 2006 February 8

## ABSTRACT

We employ a high-resolution dissipationless  $N$ -body simulation of a galaxy cluster to investigate the impact of subhalo selection on the resulting velocity distributions. Applying a lower limit on the present bound mass of subhaloes leads to high subhalo velocity dispersions compared to the diffuse dark matter (positive velocity bias) and to a considerable deviation from a Gaussian velocity distribution (kurtosis  $\sim -0.6$ ). However, if subhaloes are required to exceed a minimal mass before accretion on to the host, the velocity bias becomes negligible and the velocity distribution is close to Gaussian (kurtosis  $\sim -0.15$ ). Recently, it has been shown that the latter criterion results in subhalo samples that agree well with the observed number–density profiles of galaxies in clusters. Therefore, we argue that the velocity distributions of galaxies in clusters are essentially unbiased. The comparison of the galaxy velocity distribution and the sound speed, derived from scaling relations of X-ray observations, results in an average Mach number of 1.24. Altogether 65 per cent of the galaxies move supersonically and 8 per cent have Mach numbers larger than 2 with respect to the intracluster gas.

**Key words:** methods: numerical – galaxies: clusters: general – cosmology: theory.

## 1 INTRODUCTION

Velocity distributions in groups and clusters of galaxies can be used to determine their dynamical masses. It is commonly agreed upon that line of sight distributions similar to Gaussian reveal relaxed systems (e.g. Chincarini & Rood 1977; Halliday et al. 2004; Lokas et al. 2006). Non-Gaussianity is usually associated with merging or even multiple-merging events (e.g. Colless & Dunn 1996; Cortese et al. 2004; Adami et al. 2005; Girardi et al. 2005). Obviously, only relaxed systems may yield reliable mass estimates. However, cold dark matter (CDM) simulations have revealed high-velocity dispersions of subhaloes compared to the diffuse dark matter, even if relaxed systems are considered (Colín, Klypin & Kravtsov 2000; Ghigna et al. 2000; Diemand, Moore & Stadel 2004). In other words, the subhalo populations show a positive velocity bias or are hotter compared to the diffuse component. For dynamical mass estimates of observed clusters (e.g. Lokas et al. 2006), it is important to know whether the velocities of galaxies are biased or not.

In comparing real galaxy clusters with  $N$ -body simulations, subhaloes must be associated with galaxies. There have been different selection criteria proposed in the literature. As discussed below, the strength of the velocity bias depends strongly on the subhalo selection. Therefore, we compare the velocity distributions of two differently selected subhalo samples derived from the same  $N$ -body cluster. One sample comprises all bound dark matter substructures above a certain mass limit at present time ( $z = 0$ ). This kind of selection, which has been used in the investigations mentioned above, leads to a positive velocity bias. However, the spatial distribution of these subhaloes is less concentrated than the underlying dark

matter distribution and not in agreement with observed galaxy distributions. Diemand et al. (2004). A second subhalo sample, with distributions similar to the observed galaxy distributions, contains only those subhaloes, which exceeded a certain mass limit before accretion on to the host. Using this accretion time, subhalo selection criterion Nagai & Kravtsov (2005) were successful in matching the distribution of observed cluster galaxies with the results of  $N$ -body simulations. Conroy Wechsler & Kravtsov (2006) use the maximal circular velocity at the time of accretion to assign luminosities and stellar masses to (sub)haloes and achieve excellent agreement of modelled and observed galaxy clustering properties. This agreement suggests that the luminosity of a galaxy is related to the depth of halo potential at the epoch of high star forming activity, i.e. to its mass or circular velocity before entering the group or cluster.

Semi-analytic modelling of galaxy formation combined with high-resolution dissipationless galaxy cluster simulations (Springel et al. 2001; Gao et al. 2004) also produces similar spatial and velocity distributions for the dark matter and the galaxies. Evidently, the subhaloes populated with galaxies as in Nagai & Kravtsov (2005) but in a less transparent, more model-dependent way. Similar spatial distributions of galaxies and dark matter were also found in hydro-dynamic cosmological simulations (see Sommer-Larsen, Romeo & Portinari 2005; Nagai & Kravtsov 2005; Maccio’ et al. 2006).

The spatial distribution of tracers in cosmological dark matter haloes is related to their velocity distribution to a very good approximation via the spherical, stationary Jeans equation (Diemand et al. 2004; Diemand, Madau & Moore 2005). A spatially extended component (like subhaloes) is hotter than the dark matter whereas more concentrated subsets (like intracluster light or globular

clusters) are colder. Since cluster galaxies tend to trace the total mass distribution, one expects little or no difference between galaxy and dark matter velocity distribution. Clusters of galaxies are formed by gravitational collapse, which results in a nearly Gaussian velocity distribution for the diffuse dark component (Hoeft, Mücke & Gottlöber 2004; Hansen et al. 2006), thus the velocity distribution of galaxies should be close to Gaussian as well. In Section 2, the simulation and the two subhalo samples are described. In Section 3, we discuss the impact of the selection criterion of the subhalo samples on the velocity dispersions. Additionally, the average Mach number of galaxies orbiting in the intracluster medium (ICM) is derived. In Section 4, we summarize our results.

## 2 SIMULATION AND SUBHALO SAMPLES

We analyse a cluster-sized dark matter halo generated within a cosmological  $N$ -body simulation ( $\Omega_m = 0.268$ ,  $\Omega_\Lambda = 0.7$ ,  $\sigma_8 = 0.7$ ,  $h_{100} = 0.71$ ). The peak mass resolution is  $2.2 \times 10^7 M_\odot$  with a softening length of 1.8 kpc. The cluster ('D12' in Diemand et al. 2004) has a virial mass of  $3.1 \times 10^{14} M_\odot$  at  $z = 0$  which corresponds to  $\sim 14 \times 10^6$  particles within the virial radius of 1.7 Mpc.<sup>1</sup>

We create two different subhalo samples. On one hand, we use SKID<sup>2</sup> with a linking length of 5 kpc and identify all bound structures comprising at least 10 particles as subhaloes. This way we find 4239 subhaloes within the virial radius of the cluster at  $z = 0$ . Subsequently, this subhalo sample is referred to as sample **a**. On the other hand, we trace back the most bound particle of the subhaloes, which were identified by SKID in the same manner as mentioned above, and compare their positions with those of field haloes which are found with a friends-of-friends group finder (FOF) in earlier outputs using a linking length of 0.2 times the mean particle separation. The final sample encompasses only those subhaloes, which had progenitors (FOF field haloes) containing a minimum of 200 ( $4.4 \times 10^9 M_\odot$ ) particles at least once during their field-halo phase. In total, 367 subhaloes meet this criterion. These subhaloes are assumed to host galaxies. Nagai & Kravtsov (2005) and Conroy et al. (2006) used this approach to assign galaxies to subhaloes derived from pure dark matter  $N$ -body simulations. Subsequently, this sample is referred to as the 'galaxy sample' or sample **b**. The galaxy sample is subdivided into two subsamples according to accretion times before and after  $z = 0.15$ . The old and the young subsamples contain 174 and 193 subhaloes, respectively. We do not intend to assign any stellar properties to the subhaloes, however it is expected that the old sample represents on average redder galaxies, since star formation in these galaxies may be efficiently suppressed by interactions with the dense ICM.

Fig. 1 displays the cumulative radial number distribution for the different samples and the diffuse dark matter component. The location of the most bound particle is chosen as centre, which is assumed to coincide with the central brightest galaxy of observed clusters. We start the accumulation for all components, subhaloes, galaxies and diffuse dark matter, at 20 per cent of the virial radius ( $0.2 r_{\text{vir}}$ ). The inner 20 per cent is excluded because the high-density environment is likely to artificially remove substructure by numerical overmerging. Moreover, the survival of galaxies in this very inner region also depends on the mass distribution within their inner, baryon-dominated parts (Nagai & Kravtsov 2005; Maccio' et al.

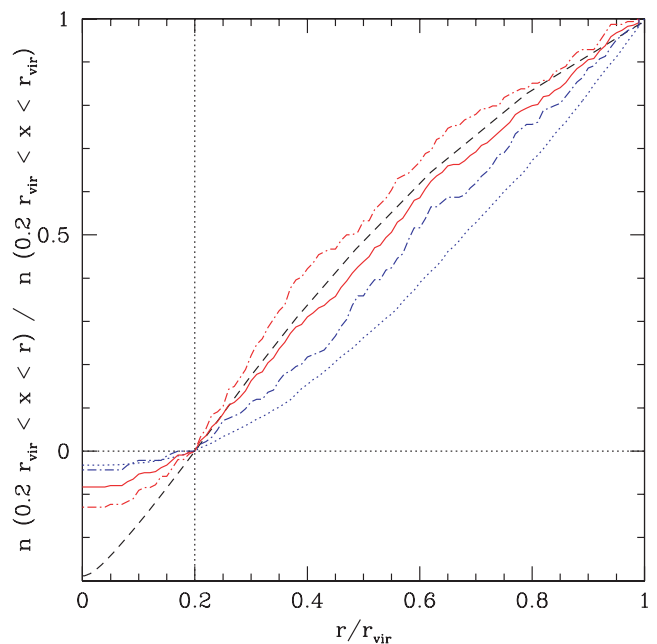


**Figure 1.** Normalized radial number distribution for the total amount of dark matter (dashed line) and subhaloes belonging to the two different samples **a** and **b** displayed in blue dotted and red solid lines, respectively. The dashed-dotted lines display subsamples of sample **b**. Red and blue colour indicates accretion before and after  $z = 0.15$ , respectively. The region within  $0.2 r_{\text{vir}}$  is excluded from accumulation to reduce the influence of numerical overmerging.

2006). The galaxy sample profile (solid line) and the diffuse dark matter profile (dashed line) are very similar, whereas the haloes of sample **a** (dotted line) show a definite deviation. The splitting of the galaxy sample according to accretion times, leads to a strongly concentrated old subsample (red dotted-dashed lines). The young subsample (blue dotted-dashed lines) is more similar to sample **a**.

The selection for sample **a** based on the current mass of the subhaloes ignores the history of the individual subhaloes. Thus, a recently accreted low-mass halo and a tidally striped old (i.e. early accreted) subhalo are treated equivalently. Due to the steep mass function of field haloes, most systems ever accreted had masses not much larger than the minimal mass. Those haloes that still lie above this minimal mass today are mostly systems which have lost little mass, i.e. recently accreted haloes in the outer part of the cluster (see Kravtsov, Gnedin & Klypin 2004; Zentner et al. 2005). The selection criterion for the galaxy sample ensures that only subhaloes with a substantial initial mass (200 particles) are counted as members of the sample. Since these haloes must have retained at least 10 particles to be found by the SKID halo finder at  $z = 0$ , they can lose 95 per cent of their initial mass on their orbits within the cluster potential well (or even more if they were more massive at the moment of accretion). The subhaloes of the galaxy sample are durable. In that respect, the galaxy sample is very similar to the diffuse dark matter component, which by default is indestructible.

## 3 DEPENDENCE OF THE VELOCITY DISTRIBUTION ON THE SUBHALO SELECTION

Fig. 2 displays radially binned velocity dispersions of the samples **a** and **b** with open and filled symbols, respectively, and the diffuse

<sup>1</sup> According to the definition used here the virial radius encloses 368 times the mean matter density.

<sup>2</sup> <http://www-hpcc.astro.washington.edu/tools/skid.html>

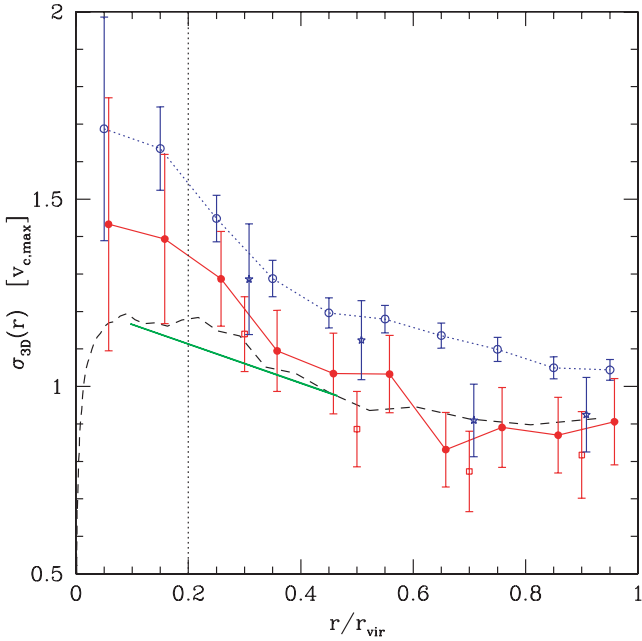


**Figure 2.** Normalized 3D velocity dispersion profiles ( $v_{c,\max} = 958 \text{ km s}^{-1}$ ) for all dark matter particles (dashed line) and haloes belonging to the subsamples **a** and **b** displayed in dotted and solid lines, respectively. The error bars display  $1\sigma$  deviations. The region within  $0.2 r_{\text{vir}}$  is likely to be affected by overmerging. Open stars and squares indicate the subdivision of sample **a** in young and old galaxies, respectively. The solid green line shows the velocity dispersion derived from X-ray temperature profiles for clusters of comparable size.

dark matter indicated by the dashed line. All dispersions are in units of the circular velocity of the host halo  $v_{c,\max} = 958 \text{ km s}^{-1}$ . The dotted vertical line marks the central region which is prone to numerical overmerging. Table 1 displays the characteristic values of the velocity distributions excluding the inner  $0.2 r_{\text{vir}}$ . The qualitative picture does not change if the central volume is included. All velocities are computed relative to the centre of mass velocity ( $v_{\text{COM}}$ ), the average velocity of all particles within  $r_{\text{vir}}$ . The dispersion of the diffuse dark matter component is shown as black dashed line. The solid green line shows the velocity dispersion derived from X-ray temperature profiles for clusters with comparable size using the relations given in Vikhlinin et al. (2005) and Evrard, Metzler & Navarro (1996).

For all radii the velocity dispersion of sample **a** deviates by more than  $\sim 15$  per cent from the diffuse component. The difference between these two distributions increases towards the centre, approaching values as large as  $\sim 30$  per cent at  $0.2 r_{\text{vir}}$ . There also appears a slight deviation of the velocity dispersion of sample **b** compared to the diffuse component, however, these deviations lie

**Table 1.** Velocity dispersion, kurtosis ( $v^4/\sigma^4 - 3$ ) and anisotropy parameter  $\beta = 1 - 0.5 \sigma_{\text{tan}}^2/\sigma_{\text{rad}}^2$  of the subhalo sample (**a**), the galaxy sample (**b**) and the diffuse dark matter (diff).

$r/[0.2, 1]$	<b>a</b>	<b>b</b>	diff
$\sigma/v_{c,\max}$	$0.665 \pm 0.007$	$0.592 \pm 0.023$	$0.5816 \pm 0.0001$
Kurtosis	$-0.61 \pm 0.16$	$-0.16 \pm 0.44$	$-0.241 \pm 0.003$
$\beta$	$-0.073 \pm 0.031$	$0.17 \pm 0.11$	$0.1103 \pm 0.0005$
$N$	4115	339	$10.9 \times 10^6$

within the  $1\sigma$  uncertainty range. The velocity dispersion profile of the galaxy sample (sample **b**) and the diffuse dark matter component are very similar. The old and recently accreted galaxy subsamples reveal lower and higher velocity dispersions, respectively. The velocity dispersions of the young subsample agree with the total galaxy sample at large radii but show excess towards the centre. Dispersions of the old galaxy subsample deviate below the total galaxy sample at large radii. The mean velocity dispersions of the subsamples compared to the velocity dispersions of all galaxy haloes are  $\sigma_{\text{old}} = 0.95\sigma_{\text{all}}$  and  $\sigma_{\text{new}} = 1.04\sigma_{\text{all}}$ .

As discussed before, the similarity of the galaxy sample and the diffuse component in the density profiles can be explained by the long lifetime of the sample members. Therefore, haloes of sample **b** can be considered as a set of durable particles similar to the simulation particles, but with much larger masses. Due to energy conservation (and without including dynamical friction or other energy redistributing mechanisms) the gravitational collapse of a distribution of different mass particles initially leads to equal velocity dispersions within different mass bins. In this scenario, neither spatial nor velocity biases are expected between sample **b** and the diffuse component. On the other hand Fig. 2 indicates a prominent velocity bias or offset between the diffuse component and sample **a**. The average lifetime of sample **a** is shorter compared to sample **b**. Sample **a** is weighted towards subhaloes that recently entered the host halo and consequently move faster. This mechanism shifts the average velocity of the remaining subhaloes in the sample towards higher values and causes a positive velocity bias (see Colin et al. 2000; Ghigna et al. 2000; Diemand et al. 2004). Fig. 3 compares the projected velocity distributions of the two subhalo samples and the diffuse component. The dotted, solid and dashed lines are the Gaussian distributions derived from the dispersions of the respective components. Table 1 displays the actual values of the velocity dispersions in units of the maximum circular velocity

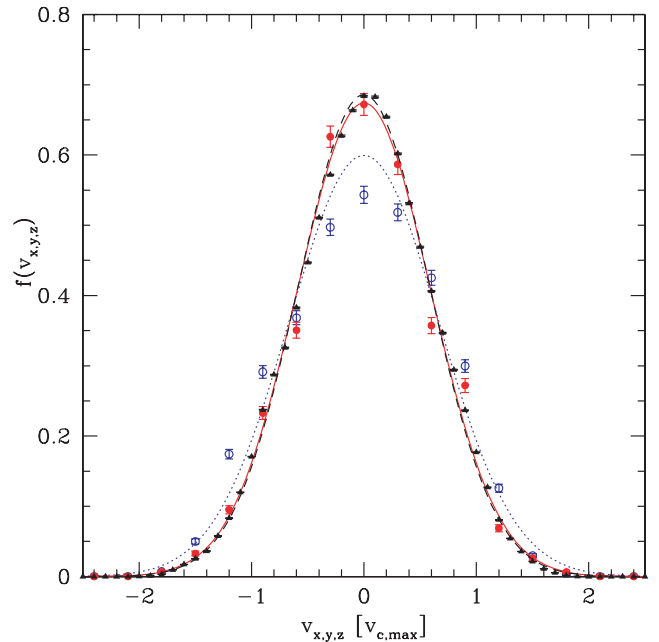


**Figure 3.** Velocity distributions of samples **a** and **b** are displayed with blue open and red filled circles. The diffuse dark matter is indicated by black triangles. The lines give the Gaussian distribution according to the mean velocity dispersion of each sample. Only objects in the range  $0.2 < r/r_{\text{vir}} < 1$  are used.

of the host halo ( $v_{c,\max} = 958 \text{ km s}^{-1}$ ). The distributions of the galaxy sample and the diffuse dark matter are very similar. The velocity dispersions and kurtosis of these two samples agree within  $1\sigma$  uncertainty. The velocity dispersion of sample **a**, however, exceeds the two others by  $\sim 15$  per cent. The corresponding velocity distribution (open circles, Fig. 3) is flat-topped and not well approximated by a Gaussian distribution (dotted line). There appears to be a lack of slow-moving subhaloes and a slight excess of high-velocity subhaloes causing a negative kurtosis of  $\sim -0.6$ . These features can naturally be explained by the loss of earlier accreted, slow-moving subhaloes due to tidal truncation. In this context, loss means decline in particle numbers below the resolution limit of 10 particles.

The shapes of observed galaxy velocity distributions in relaxed clusters can in principle be used to infer if they follow a biased, flat-topped or unbiased, Gaussian distribution. In practice this is difficult measurements since large numbers of galaxies and careful removal of interlopers are needed to achieve a significant result. There are some first hints for flat-topped velocity distributions: van der Marel et al. (2000) report a negative  $h_4 = -0.024 \pm 0.005$  (which is comparable to the subhalo samples, see Diemand et al. 2004) after stacking 16 CNOC1 clusters and excluding the cD galaxies. Lokas et al. (2006) found negative kurtosis values (around  $-0.4$ ) in five out of six nearby relaxed Abell clusters. However, the deviations from a Gaussian are only about  $1\sigma$  for these five individual systems. Our study suggests that a kurtosis which is significantly more negative than the one for the diffuse component (which has  $k \sim -0.15$ ) could be an indicator for positive velocity bias (and a related spatial antibias). It need not necessarily be related to tangential orbits (negative  $\beta$ ) as often assumed (see e.g. van der Marel et al. 2000 based on models of Gerhard 1993).

The orbital anisotropy of the galaxy sample is not significantly different from the dark matter background, both are slightly radial in cluster D12. Sample **a** on the other hand shows marginally tangential orbits. Note that there is significant variation from halo to halo in the  $\beta(r)$  profiles. The average over six relaxed clusters similar to D12 shows that the dark matter  $\beta(r)$  grows from zero (i.e. isotropic) to about 0.35 near the virial radius and total subhalo populations (corresponding to our sample **a**) show a similar behaviour with a weak tendency to be closer to isotropic on average (Diemand et al. 2004).

The green line in Fig. 2 displays the velocity dispersion (temperature) profile of X-ray gas in clusters with masses comparable to the cluster analysed here (see Vikhlinin et al. 2005). Despite all the complex gas physics involved, it is very similar to the diffuse dark matter and galaxy sample profiles. This finding can be used to estimate the typical Mach numbers of galaxies with respect to the ICM. Assuming adiabatic sound speed ( $v_s = \sqrt{\gamma\sigma_1^2}$ , where  $\sigma_1$  is the 1D velocity dispersion of the system and  $\gamma = 5/3$  is the adiabatic constant) and integrating the Gaussian distribution of the galaxies results in an average Mach number of  $\sim 1.24$ . The distribution of Mach numbers is displayed in Table 2. For supersonic galaxy motions leading bow shocks and ram-pressure stripped tails are present (Stevens, Acreman & Ponman 1999) which can be detected by X-ray observations. Tails of supersonic galaxies are expected to be more irregular than those of subsonic moving galaxies (Roediger, Brueggen & Hoeft 2006). Moreover, since ram pressure is proportional to the ICM density times the galaxy velocity squared (Gunn & Gott 1972), the appearance of leading bow shocks reduces ram pressure and decreases the stripping efficiency, which may have impact on the abundance profiles in groups and clusters.

**Table 2.** The percentage of galaxies which are expected to exceed the Mach numbers listed in the upper line.

$M \geq 1$	$M \geq 2$	$M \geq 3$
64.44 per cent	8.33 per cent	0.18 per cent

#### 4 SUMMARY AND CONCLUSIONS

Using a CDM simulation of a cluster sized ( $3.1 \times 10^{14} M_\odot$  at  $z = 0$ ) host halo, we find that different subhalo selection criteria change the resulting velocity distributions. We analyse the velocity distribution of two differently selected subhalo samples. Sample **a** contains all presently found subhaloes with masses above  $2.2 \times 10^8 M_\odot$  (10 particles). Similar selection criteria have commonly been used for investigations of the velocity bias in  $N$ -body simulations, however they do very likely not generate subhalo samples which are comparable to galaxies in groups and clusters. Sample **b** comprises subhaloes, which were able to accumulate more than 200 particles before entering the host halo. This kind of selection results in number density profiles which are similar to galaxies observed in groups and clusters (see Kravtsov et al. 2004; Nagai & Kravtsov 2005). Our main conclusions are as follows.

(1) In agreement with other authors, we find an enhancement of the velocity dispersion in the range from 15 per cent to 30 per cent if sample **a** is compared to the diffuse dark matter component. On average, sample **a** comprises more recently accreted, fast-moving subhaloes since the early accreted, somewhat more slowly moving haloes are prone to tidal dissolution. The positive velocity bias in sample **a** results from a lack of slow-moving subhaloes, i.e. a flat-topped non-Gaussian velocity distribution with negative kurtosis  $k = -0.6$ .

(2) We find no significant velocity bias between sample **b** and the diffuse component. Both have nearly Gaussian velocity distributions ( $k \sim -0.15$ ) and small radial anisotropies ( $\beta \sim 0.15$ ). Since sample **b** resembles the spatial distributions of galaxies within clusters, it seems reasonable to identify sample **b** with such galaxies. We conclude, that the velocity distribution of cluster galaxies is very similar to the underlying dark matter velocity distribution. This finding supports the assumption of not applying a spatial or velocity bias when estimating the cluster masses via galaxy kinematics (see e.g. Lokas et al. 2006).

(3) The difference between sample **a** and **b** lies in the lifetimes of the subhaloes. Many subhaloes of sample **a** are low-mass objects, lying only a little above the mass limit. If these subhaloes lose a small fraction of their mass due to tidal forces, they will no longer be members of the sample. On the other hand, members of sample **b** have to lose at least 95 per cent of their mass to be removed from the sample. Likewise, massive galaxies in clusters are assumed to survive for a long time after accretion. This can explain similar properties of the diffuse dark matter, sample **b** and luminous galaxies in clusters. However, this picture may change in smaller and/or older host systems where dynamical friction and tidal forces are more important. For instance, fossil groups are presumably old (D’Onghia et al. 2005) and may have turned a substantial fraction of their old, slow-moving satellite galaxies into diffuse intra-group light (Da Rocha & Mendes de Oliveira 2005; Faltenbacher & Mathews 2005). It is expected, that the spatial and velocity distributions of fossil groups show similar features (flattened central number-density profile and a lack of slow-moving galaxies) as found in sample **a**.

(4) The mean velocity dispersions of the whole galaxy sample compared to the old galaxy subsample differ by 5 per cent, thus the resulting mass estimates based on  $\sigma^2$  would deviate by a factor of 10 per cent. A similar trend is found in observations, if more recently accreted galaxy populations are included for the computation of the total velocity dispersion (see e.g. Mendes de Oliveira et al. 2006).

(5) We find an average Mach number of 1.24 for galaxies moving within a relaxed cluster (compare to Faltenbacher et al. 2005). Altogether 65 per cent of the galaxies move supersonically and 8 per cent show Mach numbers larger than 2. The appearance of shocks affects the interaction between galaxy and cluster gas in various ways. In particular, shocks ahead of supersonic moving galaxies reduce the ram pressure exerted on the gas in their discs.

## ACKNOWLEDGMENTS

We are grateful to William G. Mathews for insightful comments on the draft of this paper. We thank the anonymous referee who helped us to improve the original manuscript. AF has been supported by NSF grant AST 00-98351 and NASA grant NAG5-13275 and JD by the Swiss National Science Foundation for which we are very thankful.

## REFERENCES

- Adami C., Biviano A., Durret F., Mazure A., 2005, *A&A*, 443, 17  
 Chincarini G., Rood H. J., 1977, *ApJ*, 214, 351  
 Colín P., Klypin A. A., Kravtsov A. V., 2000, *ApJ*, 539, 561  
 Colless M., Dunn A. M., 1996, *ApJ*, 458, 435  
 Conroy C., Wechsler R. H., Kravtsov A. V., 2006, *ApJ*, in press (astro-ph/0512234)  
 Cortese L., Gavazzi G., Boselli A., Iglesias-Paramo J., Carrasco L., 2004, *A&A*, 425, 429  
 Da Rocha C., Mendes de Oliveira C. L., 2005, *MNRAS*, 364, 1069  
 Diemand J., Moore B., Stadel J., 2004, *MNRAS*, 352, 535  
 Diemand J., Madau P., Moore B., 2005, *MNRAS*, 364, 367  
 D’Onghia E., Sommer-Larsen J., Romeo A. D., Burkert A., Pedersen K., Portinari L., Rasmussen J., 2005, *ApJ*, 630, L109  
 Evrard A. E., Metzler C. A., Navarro J. F., 1996, *ApJ*, 469, 494  
 Faltenbacher A., Mathews W. G., 2005, *MNRAS*, 362, 498  
 Faltenbacher A., Kravtsov A. V., Nagai D., Gottlöber S., 2005, *MNRAS*, 358, 139  
 Gao L., De Lucia G., White S. D. M., Jenkins A., 2004, *MNRAS*, 352, L1  
 Gerhard O. E., 1993, *MNRAS*, 265, 213  
 Ghigna S., Moore B., Governato F., Lake G., Quinn T., Stadel J., 2000, *ApJ*, 544, 616  
 Girardi M., Demarco R., Rosati P., Borgani S., 2005, *A&A*, 442, 29  
 Gunn J. E., Gott J. R. I., 1972, *ApJ*, 176, 1  
 Halliday C. et al., 2004, *A&A*, 427, 397  
 Hansen S. H., Moore B., Zemp M., Stadel J., 2006, *J. Cosmology Astropart. Phys.*, 1, 14  
 Hoeft M., Mücke J. P., Gottlöber S., 2004, *ApJ*, 602, 162  
 Kravtsov A. V., Gnedin O. Y., Klypin A. A., 2004, *ApJ*, 609, 482  
 Lokas E. L., Wojtak R., Gottlöber S., Mamon G. A., Prada F., 2006, *MNRAS*, 367, 1463  
 Maccio’ A. V., Moore B., Stadel J., Diemand J., 2006, *MNRAS*, 366, 1526  
 Mendes de Oliveira C. L., Cypriano E. S., Sodr  L. J., 2006, *AJ*, 131, 158  
 Nagai D., Kravtsov A. V., 2005, *ApJ*, 618, 557  
 Roediger E., Brueggen M., Hoeft M., 2006, *MNRAS*, submitted (astro-ph/0603565)  
 Sommer-Larsen J., Romeo A. D., Portinari L., 2005, *MNRAS*, 357, 478  
 Springel V., White S. D. M., Tormen G., Kauffmann G., 2001, *MNRAS*, 328, 726  
 Stevens I. R., Acreman D. M., Ponman T. J., 1999, *MNRAS*, 310, 663  
 van der Marel R. P., Magorrian J., Carlberg R. G., Yee H. K. C., Ellingson E., 2000, *AJ*, 119, 2038  
 Vikhlinin A., Markevitch M., Murray S. S., Jones C., Forman W., Van Speybroeck L., 2005, *ApJ*, 628, 655  
 Zentner A. R., Berlind A. A., Bullock J. S., Kravtsov A. V., Wechsler R. H., 2005, *ApJ*, 624, 505

This paper has been typeset from a  $\text{\TeX}/\text{\LaTeX}$  file prepared by the author.